minerals

MDPI

Article

Characteristics and Geological Significance of High-Frequency Cycles in Salinized Lake Basins: The Paleogene Kumugeliemu Group in the Xinhe Area, Northern Tarim Basin

Yanru Yang [1,2], Jingchun Tian [1,2,*], Xiang Zhang [1,2], Yingxu Li [3], Yue Zhang [1,2] and Qiaoyi Xia [1,2]

[1] State Key Laboratory of Oil and Gas Reservoir Geology and Exploitation, Chengdu University of Technology, Chengdu 610059, China; 17761246967@163.com (Y.Y.); zhangxiang06@cdut.edu.cn (X.Z.); zly077y@163.com (Y.Z.); 18200596359@163.com (Q.X.)
[2] State Key Laboratory of Oil and Gas Reservoir Geology and Development Engineering, Chengdu University of Technology, Chengdu 610059, China
[3] BGP Inc., China National Petroleum Corporation Southwest Geophysical Institute, Chengdu 610041, China; lyx16639529085@163.com
* Correspondence: tjc@cdut.edu.cn

Abstract: Salinized lake basins have distinctive sedimentary response characteristics, similar to marine shallow-water carbonate platforms. High-frequency cycles can also be used to reveal more sedimentological information, such as relative lake-level fluctuations, lithofacies sequence combinations, and paleogeographic evolution. In this article, a comprehensive study on the stratigraphic shelf delineation and high-frequency cycles of the Paleozoic Kumugeliemu Group in Xinhe area, northern Tarim Basin, was performed using drilling cores, logging curves, and seismic analyses. As a result of the study, the following data were obtained: the three sets of marker beds in the Kumugeliemu Group in the study area could be divided into a bottom sandstone component ($E_{1\text{-}2}$ km^1), a lower gypsum mudstone component ($E_{1\text{-}2}$ km^2), a salt rock component ($E_{1\text{-}2}$ km^3), and an upper gypsum mudstone component ($E_{1\text{-}2}$ km^4) by petrology vertical overlay combination and isochronous tracking correlation, which constituted two third-order cycles (ESQ_1, ESQ_2). They were further divided into seven fourth-order cycles (Esq1–Esq7). Due to the droughty and saline lacustrine depositional system background, the internal rock fabric changed frequently and showed a periodic vertical overlay pattern. Stratified gypsum salt, gypsum mud (sand) rock, and gypsum rock were used as the cycle interface. A single cycle was mainly characterized by an upward shallower depositional sequence of rapid lake transgression followed by a slow lake regression, composed of massive sandstone–lamellar mudstone–lime dolomite–gypsum rock, massive sandstone–lamellar mudstone–gypsum rock (gypsum salt), massive sandstone–massive gypsum mud (sand) rock–gypsum rock, and other cycle structure types. The complete sedimentary cycle was superposed by a single cycle and compared by the inter-well thickness difference, indicating that the study area had a paleogeomorphology pattern of "West-Low–East-High". The thickness of the cycles decreased gradually from bottom to top vertically, and five sedimentary stages were determined, i.e., freshwater, brackish, brackish water, salt lake, and semi-saltwater, reflecting the evolutionary process of increasing salinity, lake basin filling, and gradual salinization and shrinkage.

Keywords: lake-level fluctuation; high-frequency cycles; salinized lake basin; lake transgression-regression; Kumugeliemu Group in the Xinhe area

Citation: Yang, Y.; Tian, J.; Zhang, X.; Li, Y.; Zhang, Y.; Xia, Q. Characteristics and Geological Significance of High-Frequency Cycles in Salinized Lake Basins: The Paleogene Kumugeliemu Group in the Xinhe Area, Northern Tarim Basin. *Minerals* **2023**, *13*, 824. https://doi.org/10.3390/min13060824

Academic Editor: Santanu Banerjee

Received: 22 May 2023
Revised: 13 June 2023
Accepted: 14 June 2023
Published: 16 June 2023

1. Introduction

Terrestrial saline lake basins are sedimentary environments with droughty, hot, and unique depositional patterns and are an important research object of study for sedimentological interpretation [1]. Moreover, changes in sedimentation and reservoir formation

characteristics caused by lake-level fluctuations are often inextricably linked to hydrocarbon resources and one of the main influencing factors of lithologic oil reservoirs, thus garnering extensive attention from researchers on hydrocarbon exploration [2–6]. In China, terrestrial saline lake basins are mainly developed in Cenozoic intermountain basins, such as the Lower Ganchaigou Formation in the Qaidam Basin [4–6], the Shahejie Formation in the Dongying Depression [7,8], and the Kumugrem Group and Suweiyi Formation in the Tarim Basin [9–12], all of which have similar depositional characteristics. Several scholars have studied the regions to varying degrees. Frequent changes in the lake level in terrestrial saline lake basins because of structure factors and climatic conditions are the core factors resulting in lake basin salinization [5] and changes in sedimentary products, influencing the relationship between supply and accommodation space, while the sedimentary cycle features recorded in the geological–historical period are the product of the combined effect of structure movements and paleoclimate [4,11–14]. Therefore, the products of high-frequency cycle deposition are an important representation of the paleogeomorphology and paleoclimatic conditions responding to the characteristics of terrestrial saline lake basins.

The Cenozoic Paleogene deposits are extensively distributed throughout the Tarim Basin, with a particular concentration in the Tabei Uplift area [15]. Due to structure movements and paleoclimatic conditions, a broad and shallow lake deposit was formed [16], with a typical "north-sinking, south-rising" structure pattern [9,17,18]. Because of the discovery of the Yudong 1 well lithological trap in the Wensu area [19] and the Kra 2 gas field as the main resources for the "West–East Gas Transmission" project in China [20], most scholars have successfully focused their research on the depositional environment, sequence stratigraphy, and reservoir formation of the Paleocene system in the perimeter of the Wensu Bulge and the Kuqa Depression. However, there has been scarce literature on the recovery of high-frequency cycles and paleogeographic patterns caused by structure movements and paleoclimatic conditions, particularly in the Xinhe area. With new technologies for oil and gas development and exploration technologies and the use of the XH5 well for maximizing production capacity benefits, the exploration and development of the Xinhe area have increased in recent years. Based on this, through the interpretation and analysis of drilling and logging coring data, logging curve characteristics, 2D and 3D seismic data for the Xinhe area, the diachrony of the lithologic section [21], and the inheritance of the marker bed [22]—combined with the evaluation of the geological background, the regional paleoclimate environment, and previous studies on adjacent areas—the identification and division of the fourth-order sequence boundaries in the study area were comprehensively analyzed, and the sedimentary cycle characteristics were controlled by the lake-level rise and fall. It is hoped that this study will further encourage the exploration of the sedimentary stages and evolution characteristics of lake basins, enriching our knowledge of continental saline lake basin sedimentary cycles in China, and provide a theoretical basis for subsequent oil and gas exploration and paleo sedimentary pattern research.

2. Geological Setting

2.1. Geological Location, Tectonics, and Stratigraphy

The Tarim Basin is a large, superimposed basin in western China, covering an area of about 500,000 km^2 [23]. It is characterized by an ancient crystalline basement and a thick sedimentary cover and is considered one of the three major cratons in China [24]. Distinguished by fault system and structural stratigraphy characteristics, the Tarim Basin can be described as a structural unit of "three uplifts and four depressions" [25–28].

The Xinhe area of the Tarim Basin is part of the Tabei Uplift Structure, which is a superimposed paleo-uplift with a gradual intrusion of strata from east to west with a morphological distribution of "four uplifts and two depressions" (Yingmaili low Uplift, Wensu Uplift, Lunnan low Uplift, and Korla nasal Uplift) [29,30]. The structure evolved through three stages: the Late Garidon–Early Haixi period of stable uplift and denudation, the Late Haixi–Indo-Chinese period of extrusion and uplift, and the Yanshan–Xishan period of adjustment and definition. In the Cenozoic a collision of the Indo–European

plates occurred, which uplifted the Tibetan plateau, making the evolution of the whole basin most strongly influenced by structural elements [31] and subjecting it to multiple stages of structure movements. In this region, the structure evolution of the study area is characterized by curtain-like subsidence. The main body of the study area is located in the Shaya Uplift above the Tabei Uplift, which is adjacent to the Kuche Depression to the north, belongs to the Yakla Fault convexity to the south, and is connected to the Shaxi Uplift to the west, straddling the combined part of the Kuche Depression and the Shaya Uplift at the northern margin of the Tarim Basin [32,33] (Figure 1a,b).

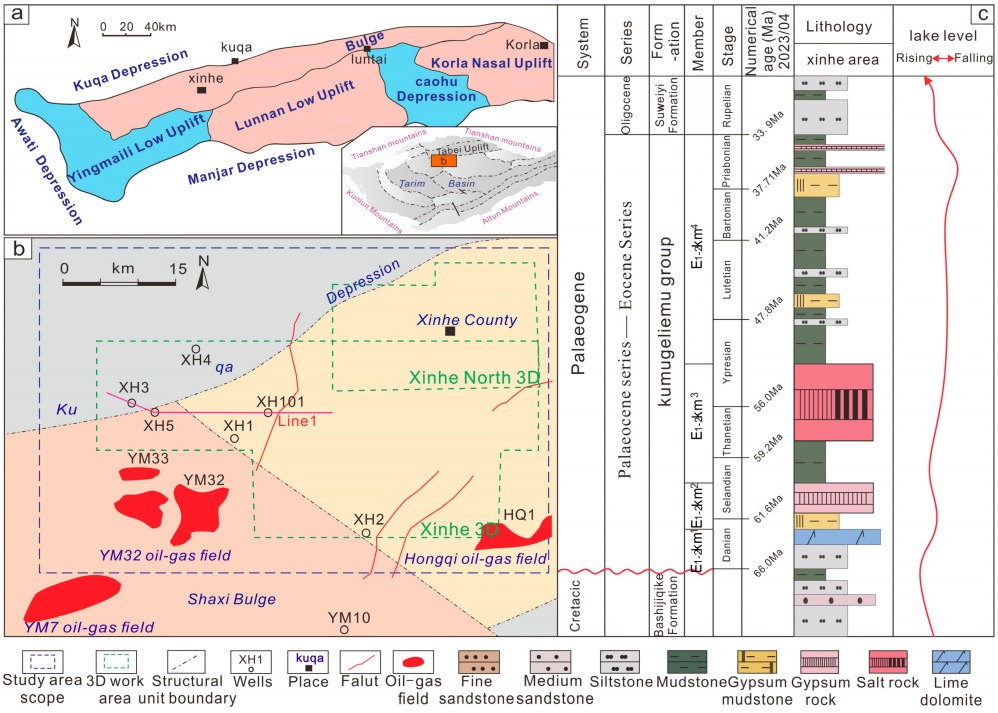

Figure 1. Structural location and stratigraphic development characteristics of the study area. (**a**) Structural location map of the Tabei Uplift (according to [9,10], revised); (**b**) study area location (according to [33], revised); (**c**) comprehensive stratigraphic column of the study area. (The numerical age is quoted from the international chronostratigraphic map issued by the International Commission on Stratigraphy in April 2023 [34].

2.2. Stratigraphy and Sedimentary Environment

The Paleogene system was formed between the middle and the late Himalayan period, during a long uplift. A continuous uplift in stages led to high paleo-altitude, dry climate, and closed basins resulting in increasing salinity, forming a typical salinized lake basin belonging to the river–lake phase sedimentary system [35]. The Kumugeliemu Group develops in the study area, with thickness ranging between 100 and 300 m, angular unconformable contact with the underlying formation, and integrated contact with the overlying Suweiyi Formation. From previous studies, the bottom-to-top development of massive sandstone, paste mudstone (sand), gypsum rock, and paste salt lithology vertical superposition features can be classified into bottom sandstone ($E_{1\text{-}2}$ km^1), lower gypsum mudstone ($E_{1\text{-}2}$ km^2), gypsum salt ($E_{1\text{-}2}$ km^3), and upper gypsum mudstone ($E_{1\text{-}2}$ km^4) [9] (Figure 1c).

3. Materials and Methods

Data from ten drilling sites in the Xinhe area and adjacent areas were selected to determine the high-frequency sequence cycle interface, including core thin sections, drilling lithology records, logging curve data, two-dimensional (2D) seismic profiles, and three-dimensional (3D) seismic work areas. The drilling sites were all affected by large fault

structures, and stratigraphic overlaps formed. All the data were provided by the Exploration and Development Research Institute of Sinopec Northwest Oil field (Figure 1).

3.1. Seismic Data

Seismic data were collected using 2D seismic lines in the Xinhe area of the Tabei Uplift within the permission of Sinopec. Through the diffusion filtering processing of 2D seismic data, the quality of the merged seismic data volume was improved, the block transition was natural, the layers were coordinated, and the energy was more balanced. The typical representative in this study is Line1 (seismic profile DYWE238) 2D (Figure 2), and the stratigraphic division of the study area was determined to establish three sets of marker layers and provide the seismic response characteristics and other seismic information. A 3D seismic survey of the database of Sinopec using the Exploration Geophysicists Association standard provided positive (peak) reflection events in terms of the increase of wave impedance. The 3D work area of the research area comprised the Xinhe 3D and Xinhe North 3D overlays, with seismic data covering approximately 741 km^2. All seismic profiles were interpreted with LandMark2005 software on an HP xw6600 workstation, and all seismic profiles were offset profiles.

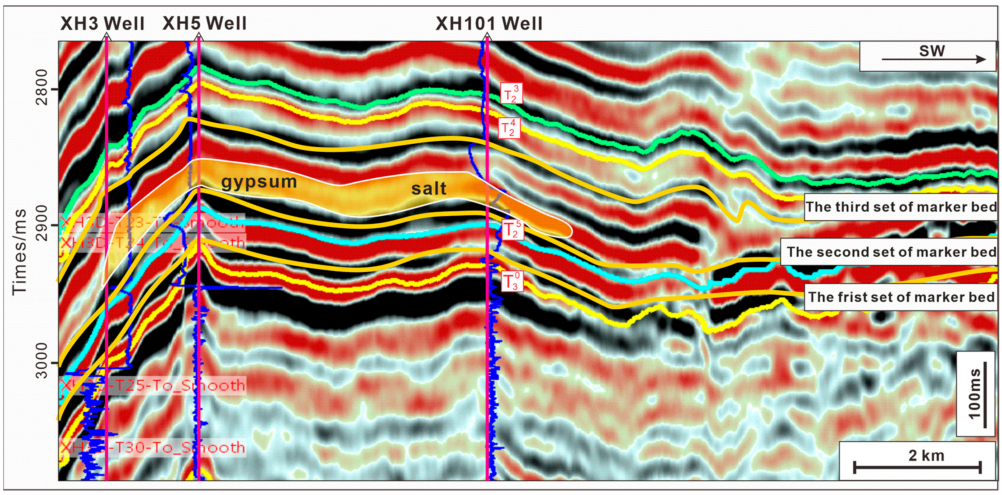

Figure 2. Southwest–northeast seismic section of the XH3–XH101 wells in the Xinhe area.

3.2. Logging and Core Data

The core logging data were obtained from the database of the Exploration and Development Research Institute of Sinopec Northwest Oil field. To record while drilling, the lithology of the Kumugeliemu Group was selected for depth correction, and a total of 2970.6 m of lithology logging correction was completed. The logging data chosen in the database were the GR, AC, SP, and RD logging curves, and the interpretation point was 0.125 m. The lithology logging and logging data were processed with resfrom3.0 software developed by Kaben Company, and outlier were removed by correction of the logging curve depth. A total of 9000 m of curve data was determined.

The Exploration and Development Research Institute of Sinopec Northwest Oil field provided the core thin sections of the coring well section. Samples were taken from 10 drilling research layers in the Xinhe area by the split core sampling method at a 1.5 m. sampling interval in accordance with the "General Rules and General Provisions for Chemical Analysis of Rocks and Ores in the National Standard of the People's Republic of China (GB/T14505-2010)". An SYJ-200 automatic precision cutting machine was used, as well as a UNIPOL-1202 automatic precision grinder, a GPC-80A precision grinding and polishing control instrument, an MTI-3040 heating platform, and a DZF-6020 vacuum drying oven. Moreover, the Exploration and Development Research Institute of Sinopec Northwest Oil Field performed the thin film production. Rock thin section identification was performed at the Institute of Sedimentary Geology, Chengdu University of Technology, in accordance

with the Technical Specification for Rock and Mineral Identification in the Geological and Mineral Industry Standards of the People's Republic of China DZ/T0275.1-2015, using an optical microscope (Nikon E600 POL, Tokyo, Japan).

3.3. Research Methods

By utilizing drilling core data, well logging curves, and the vertical lithological combination characteristics of the Xinhe area, three sets of isochronous traceable marker beds were established. The establishment of these marker beds provided a crucial foundation for in-depth investigations into the geological history and sedimentary evolution of the study area. Through the analysis of the seismic profile characteristics, the top and bottom boundaries of the Kumugeliemu Group were identified as unconformity interfaces, denoted as T_2^4 and T_3^0, respectively. These interfaces can be continuously traced in seismic data and exhibit similar continuity features as the neighboring Wensu ancient uplift. These unconformity interfaces play a significant controlling role in the formation and development of two third-order sequences (ESQ_1 and ESQ_2). Based on the lithological interface characteristics observed through the drilling core data and thin section analysis, along with the integration of well–seismic data correlation, seven fourth-order sequences (Esq1–Esq7) were successfully identified within the constraints of the third-order sequences. By examining the lithological combination and thin sections of the drilling cores, four typical single-cycle sequences were further delineated, reflecting the sedimentary infilling processes in the study area. Simultaneously, through the comparison of the high-frequency cycles between wells, important information regarding paleogeographic features and basin floor morphologies in the study area was reconstructed. Furthermore, by analyzing the three-dimensional seismic facies map and the tectonic evolution features of the basin and considering the coupled relationship between sediment provenance direction, tectonic movements, and climate, a basin evolution model for the Kumugeliemu Group during the study period was established. This model provides significant guidance for a better understanding of the geological evolution processes in the study area. Through the comprehensive application of various geological investigation methods, stratigraphic correlation marker layers were successfully established, sequence characteristics were identified, and in-depth studies on sedimentary infilling processes and basin evolution patterns in the study area were conducted. These findings provide robust support for the in-depth interpretation of the geological history and sedimentary environment of the area.

4. Results

4.1. Layer Sequence Interface Identification

The sedimentary sequence was established based on the sedimentary cycle generated by changes in the sea and lake levels and the identification of the maximum amounts of water receding or entering the traced interface; each sedimentary cycle allowed establishing a level of the sequence [35]. The lithology transition surface can be used as a main basis for the delineation of the stratigraphic sequence, and the isochronous marker bed is used as the core of the stratigraphic isochronous trace comparison [9]. Using the drilling and logging data, the logging curves, and the seismic data for the study area, a high-frequency stratigraphic framework of the study area was established according to the identification of the isochronous marker bed and interfaces in the third-order sequence.

4.1.1. Marker Beds

Due to their obvious regional characteristics and stable distribution, wide distribution, continuity, and easy identification, marker beds can be used as a small-scale regional comparison layer [9,22]. A series of three sets of marker beds were identified in the Paleozoic Kumugeliemu Group in the Xinhe area, with stable distribution and region-wide contrast. The upper part of the Kumugeliemu Group comprised the third set of marker beds, with a lithology of mainly gypsum mudstone and mudstone and high GR and low RD characteristics. The second set of markers in the middle part had a lithology of mainly

gypsum–salt, was the one most influenced by variations of the lake level among the three sets of marker beds, had low GR and high RD and strong continuous seismic reflection, and showed cross-merging with the same phase axis and reflection characteristics of salt rock (Figure 2). The lower part, with the first set of marker beds, was mainly characterized by low-GR and high-RD lime dolomite (Figure 3).

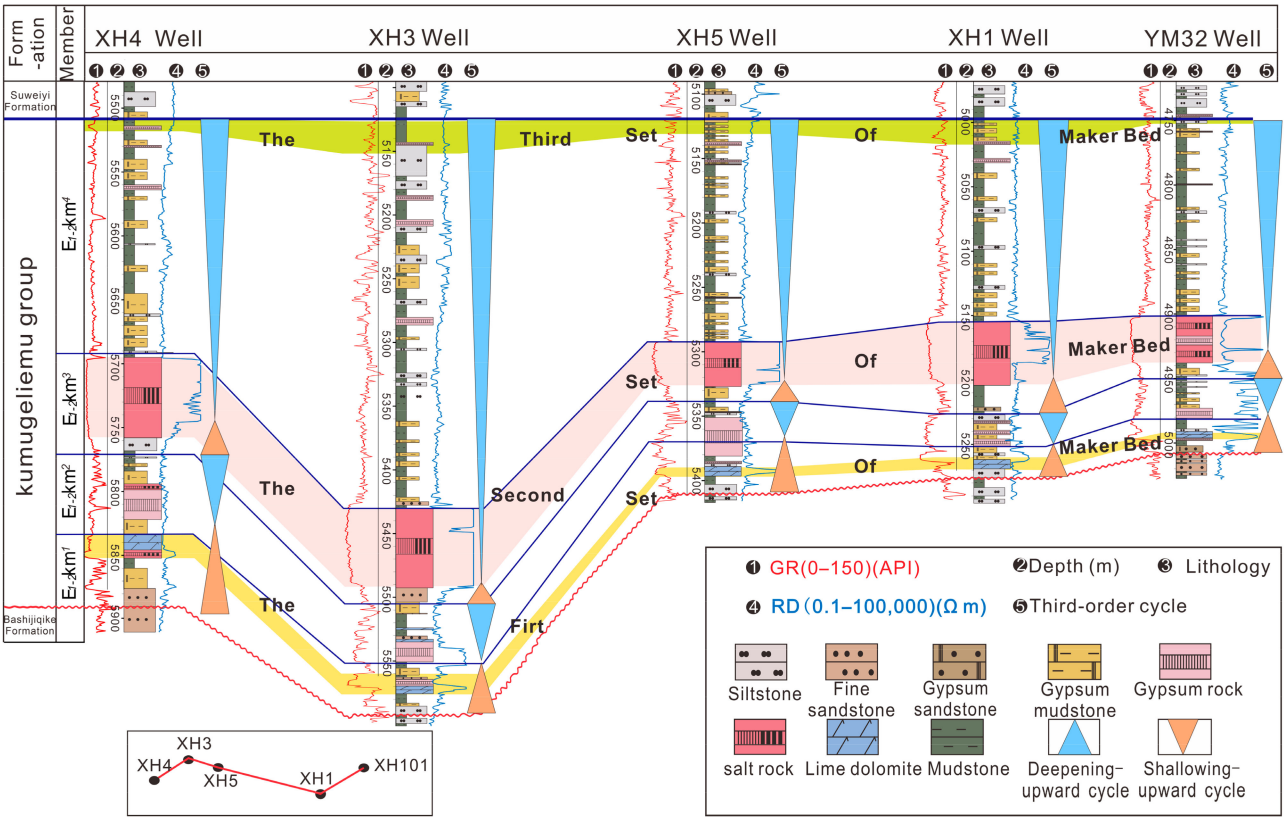

Figure 3. Profile map of connecting XH4–YM32 wells in the southwest–northeast direction of the marker layer in the Xinhe area.

4.1.2. Third-Order Sequence Boundary

From the seismic profile characteristics, the top and bottom of the Kumugeliemu Group had an unconformity surface indicated by T_3^0 and T_2^4, both of which could be traced continuously on the seismic profile. Due to the limited seismic data, they are shown to be close to the central area of the basin, and two interfaces correspond to the third-order sequence boundary with integrated contacts and locally visible concordant surfaces (Figure 2). Researchers [9] found the same three sets of marker beds in the neighboring area of Wensu-Yingmaili, and the seismic profiles had the same characteristics, such as continuity, as those in the Xinhe area. Combined with the characteristics of regional tectonic evolution, it is considered that the two areas have continuity, and the third-order sequence division has the same characteristics. The ESQ_1 sedimentary period was mainly controlled by T_3^0 and the bottom of the second set of marker beds, where the largest lake flooding surface is located in the middle mudstone with high GR and low RD in the lower gypsum mudstone between the second and the third marker beds, which is a combination of the bottom sandstone component (E_{1-2} km^1) and the lower gypsum mudstone component (E_{1-2} km^2). The ESQ_2 depositional period was mainly controlled by the bottom of the second set of marker beds and T_2^4, and appeared to be a combination of salt rock (E_{1-2} km^3) and upper gypsum mudstone (E_{1-2} km^4) (Figure 3).

4.1.3. Fourth-Order Sequence Boundary

The fourth-order sequence boundary is the intersection formed by the shallowest water body at the top of each cycle and the deepest water body environment at the beginning of the next cycle [5]. Due to the limited resolution of the 2D seismic logs in the study area, the seismic logs were combined with the lithological characteristics, as well as with the logging curves and other information for a comprehensive analysis. This boundary mainly included the surface of the conversion of gypsum formation or gypsum mud (sand) stone to pure clastic rock, the interface of the conversion of salt rock to clastic rock, and the interface with the characteristics of a small local scouring surface. The logging curve mainly reflected the variation of the GR value from low to high and of the RD value from high to low and the increase in mud content, all of which represented the conversion surface of the sudden deepening of the water body (Figure 4). A total of eight stratigraphic interfaces, namely, ESB_1, ESB_2, ESB_3, ESB_4, ESB_5, ESB_6, ESB_7, and ESB_8, were identified in the Kumugeliemu Group in the Xinhe area, and system domains were proximally divided.

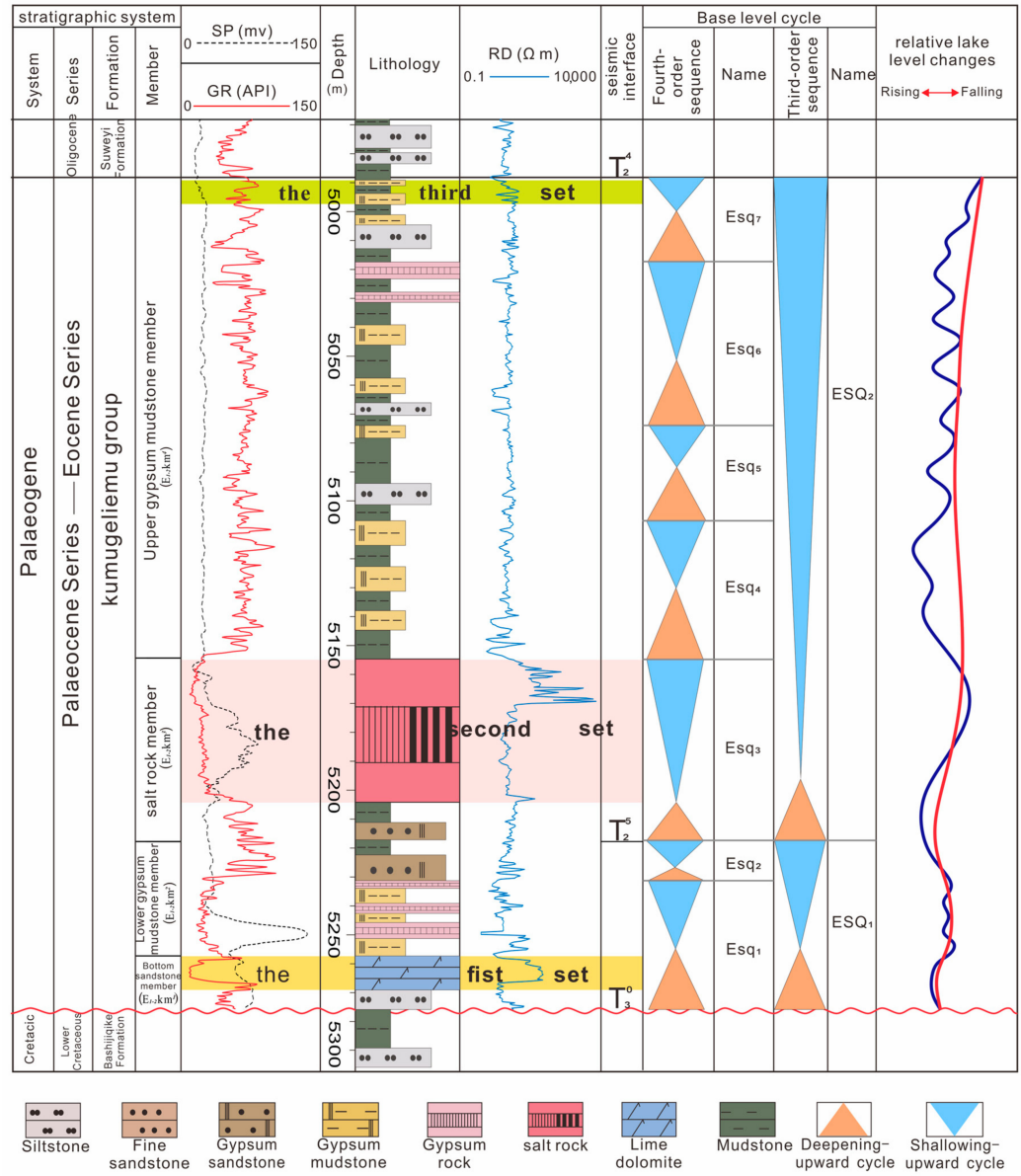

Figure 4. Lithology, lake-level fluctuation, and cycle divisions of the Paleoproterozoic Kumugeliemu Group in the XH1 well, Xinhe area.

4.2. Fourth-Order Sequence Division

Two third-order sequences were identified within the Paleozoic Kumugeliemu Group in the Xinhe area based on the interface characteristics and the combined logging and seismic data. For example, the bottom sandstone member in the XH1 well (Figure 3) appeared to be a low-stand systems tract (LST) of the ESQ_1 period, mainly composed of positive-graded medium and thick bedding fine sandstone with thin bedding mudstone and lime dolomite interbedded deposits, and its GR curve was a combination of a funnel-shape curve and a box-shaped curve. The middle and lower parts of the lower paste mudstone component appeared to be lake transgressive systems tract (TST), mainly composed of thin-bedding mudstone and paste mudstone; the upper member, i.e., the high-stand systems tract (HST), mainly consisted of deposited interbedded gypsum rocks and creamy mud (sand) rocks.

However, not all lithologies appeared to be fully developed. Except for the development of limy dolomite in the middle and lower parts of Esq1, the absence of carbonate was observed in the deposition period of Esq2–Esq7, indicating a deeper water body in the period of Esq1 than in other periods. During the deposition of the Paleozoic Kumugeliemu Group in the study area, the general climate was relatively droughty, and the lake level was relatively low, locally characterized by rapid lake transgression and relatively small rises in the lake level. Following the evolution of the lake basin, the salinity increased and the climatic conditions for the development of the gypsum salt bed were established (Figure 4).

4.3. Types and Characteristics of the High-Frequency Cycle Sequences

Drill cores and thin sections observation (Figure 5), together with the above macroscopic characteristics and the regional sedimentary environment evolution, showed that there were obvious differences between the wells, which were controlled by the variable characteristics of the rock components, the structural yield, the hydrodynamic energy magnitude, and the lake salinity caused by alternating paleoenvironmental replacements and frequent changes in the lake levels. There were obvious variable changes in the rock components, structure yield, hydrodynamic energy magnitude, and lake salinity within the inner cycle and between different wells, which were controlled by alternating paleogeomorphology changes and frequent changes in the lake levels. These changes were often controlled by frequent lake-level fluctuation, and were ultimately evident in the sedimentary record in terms of changes in rock yield, evaporative mineral content, etc. Based on the above features and the fourth-order cycle, it was found that the Kumugeliemu Group in the study area is subject to frequent lake-level fluctuations in the vertical direction, which leads to the overlaying of a variety of rock types and comprises a variety of complete or incomplete upward-varying shallow cycle sequences. Combined with the sedimentary features and the environment evolution, the following four typical single-cycle sequences were identified.

4.3.1. Cycle Sequence I

The sequence from the bottom to the upper level consisted of siltstone, laminated mudstone, lime dolomite, and gypsum rock (Figure 6 (I)). The set of the cycles mainly developed in the lower part, and the bottom was little affected by the lake wave action due to weak hydrodynamic conditions during the initial lake intrusion. The main deposit was positive-grain-order massive siltstone (Figure 6 (I-1,2)), about 3.55 m thick, with an uneven scour surface and presented unconformity contact with the underlying formation (Figure 5a). With the deepening of the water body, grainy laminated mudstone was deposited rapidly near the maximum lake flood surface (Figure 6 (I-3,4)), and a few carbonate particles were sedimented (Figures 5b and 6 (I-4,5)). Subsequently, the lake became shallower, and sedimentation in the first carbonate marker bed began, which was about 0.5–2.25 m thick (Figure 6 (I-5)). By comparison of the marker beds, it was found that the carbonate rock marker bed thinned toward the lake basin, occasionally showing a thin and clastic rock-interbedded sedimentary layer, reflecting the overall shallowing of the

lake, but the internal water body was more turbulent, with a few paste masses occurring occasionally in the sandstone and mudstone (Figure 5c). With a further decline of the lake level, the salinity gradually increased with the shallowing of the water body. Sulfate rocks started to precipitate in this period, sedimenting large amounts of gypsum that formed a gypsum bed, with brecciaous gypsum appearing at the top; this was also the shallowest part of this cycle of the water body (Figure 6 (I-6,7)).

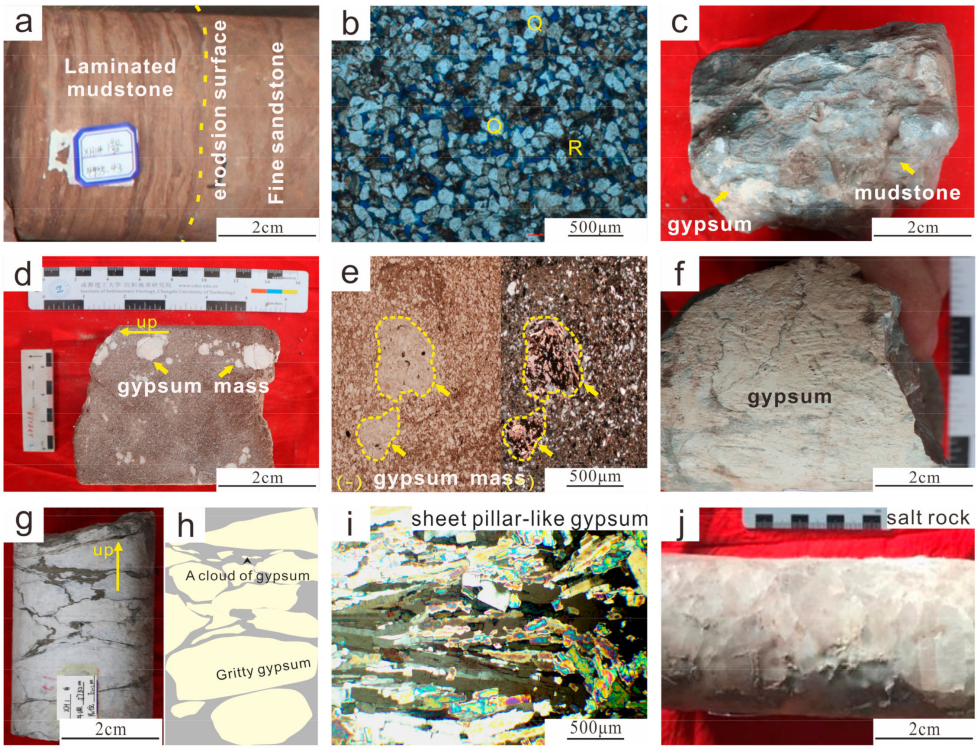

Figure 5. Macro and micro rock characteristics of the Kumugeliemu Group in the Xinhe area. (**a**) XH3 well, 5583.15 m. The lower part is positive-grain-order siltstone, while the upper part is laminated mudstone with a scouring surface; (**b**) XH3 well, 5583.15 m, fine-grained feldspar chip siltstone, with cloudy, lime colloid and the development of a few intergranular lysis pores (-); (**c**) XH3 well, 5565.5 m, gray-green massive gypsum mudstone; (**d**) XH1 well, 5218.5 m, brown gypsum fine sandstone. Localized gypsum mass with directional arrangement; (**e**) XH3 well, 5211 m, gypsum siltstone with a gypsum mass and clay matrix development; (**f**) XH3 well, 5220 m, gray-green gypsum mudstone; (**g**) XH1 well, 5172 m, off-white gypsum salt; (**h**) sketches, with agglomerate, cloudy gypsum and a laminated structure development, upward, the gypsum mass appears torn; (**i**) XH3 well, 5207 m, gypsum rock, sheet pillar-like gypsum, with local development of a small amount of sand (+); (**j**) XH1 well, 5156 m, salt rock.

4.3.2. Cycle Sequence II

This sequence was mainly composed of siltstone, thinly laminated mudstone, and gypsum mudstone (gypsum sandstone) (Figures 6 (II) and 7 (II)). The rock assemblage was relatively simple, mainly developed in the middle and upper parts of the lower gypsum–mudstone component, with a thin single lamina thickness between 0.8 and 2 m (Figures 6 (II-8,9,10) and 7 (II-3,4)). The siltstone with a positive-graded sequence at the bottom formed a high-frequency cycle interface with the evaporite-solution breccia at the top of the cycle sequence I (Figure 7 (II-1,2)). The overall water body of this sequence was quiet and deep, and the interior was less influenced by lake transgression-lake regression processes. The main material was supplied by river water, and most of it showed a thin bed; the top paste masses were small, but showed a directional arrangement without fragmentation (Figure 5d,e).

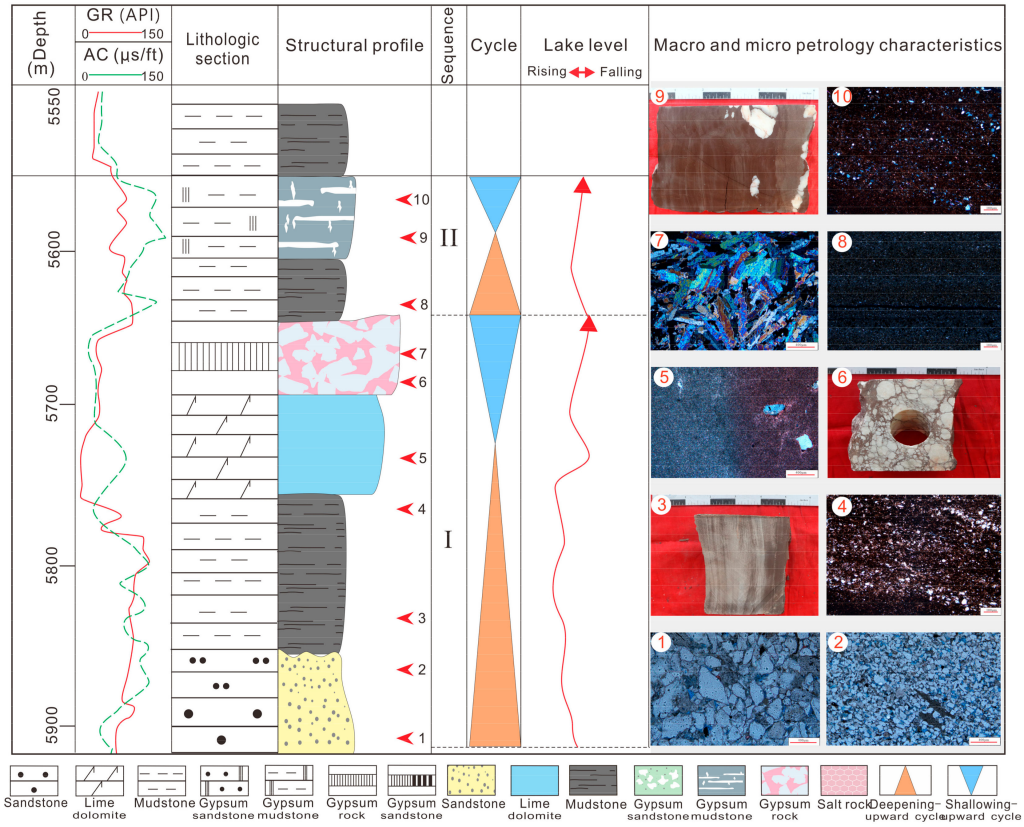

Figure 6. Typical assemblies in the vertical cycle sequences I and II of the Kumugeliemu Group (XH3 Well, 5557.8–5901.2 m) in the Xinhe area.

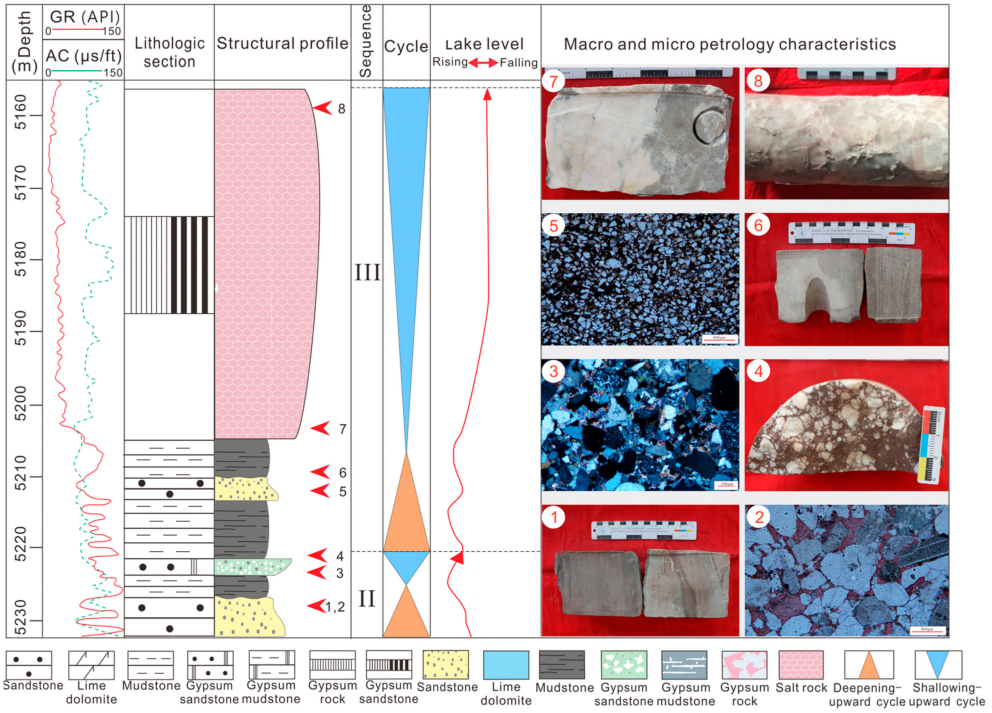

Figure 7. Typical assemblies in the vertical cycle sequences II and III of the Kumugeliemu Group (XH1 Well, 5158.5–5232 m) in the Xinhe area.

4.3.3. Cycle Sequence III

This sequence was composed of clastic rock–gypsum salt (Figure 7 (III)). It was the thickest single cycle in all the cycles, with thickness between 30 and 40 m. The lithologic interface between the massive mudstone and the underlying paste (mud) sandstone was the second high-frequency cycle interface (Figure 7 (III-5,6)), showing local rapid lake transgression and sudden deepening of the water body, constituting a transient deposition process of the massive mudstone–siltstone. As the lake level declined, the sedimentary water body became shallower. Large amounts of sulfate minerals such as calcium mannite and gypsum–anhydrite rock began to deposit, salinity continued to increase, and the lake basin developed toward a salt lake. In the context of a hot, droughty evaporative climate, the salinity of the lake basin area increased due to the sheltering effect of the surrounding geomorphic uplands in the study area. The high salinity brine converged continuously downward with gravitational deposition and produced the gypsum–salt rock in a bedded form below the wave base, in a relatively low-energy, hydrostatic environment (Figures 5g,h and 7 (III-7)). As the salt rocks were easily damaged, some were stripped to form block salt rocks during drilling (Figures 5j and 7 (III-8)).

4.3.4. Cycle Sequence IV

Consisting mainly of clastic rock and gypsum, this sequence was the most widely developed sedimentary sequence in the study area. The bottom positive-grain-order siltstone formed a third cycle interface with the underlying laminated gypsum–salt (Figure 8 (IV_1-1,2)). The cycle sequence experienced rapid lake transgression and deepening of the water body. Sedimentary material was carried by the river into the lake basin to form massive siltstones (Figure 8 (IV_1)), but sometimes the water body was less energetic and carried clay minerals to form massive mudstones (Figure 8 (IV_2)). With the relative decline of the lake level, the water body became shallow, evaporation was enhanced, salinity increased, massive gypsum mudstone and gypsum siltstone were formed (Figures 5f and 8 (IV_1-3,4,5,IV_2-7)), and the gypsum content relatively increased compared with that in the lower gypsum mudstone. As the lake level continued to decline and salinity increased, heavy brine continued to seep down, and recrystallization occurred, leading to a laminated gypsum (Figures 5i and 8 (IV_1-6,IV_2-8)). Sequence IV can be divided into two types based on the magnitude of the hydrodynamic conditions at the bottom, both of which reflect a shallowing of the water body from the bottom up, a dry and hot climate, and a gradual increase in salinity (Figure 8).

The above four typical single cycles have common characteristics, namely, a sudden deepening of water body, a rapid rise in the lake level and a decrease in salinity at the beginning of each cycle deposition, and the beginning of clastic rock development, followed by shallowing and increased salinity of the lake water and the development of a large amount of gypsum–anhydrite rock and calcium mannite. Besides the four complete typical cycle sequences mentioned above, other incomplete cycle structures were observed: the II and IV cycle sequences widely developed in the lower and upper parts of the cycle, and the single cycles showed a rapid transgression–slow lake regression deposition; the rock yield and composition also showed cyclonic variation characteristics. Such a sedimentary process has some formation significance [36], and thus, vertical building and inter-well comparison of the high-frequency cycles of the Kumugeliemu Group were further studied.

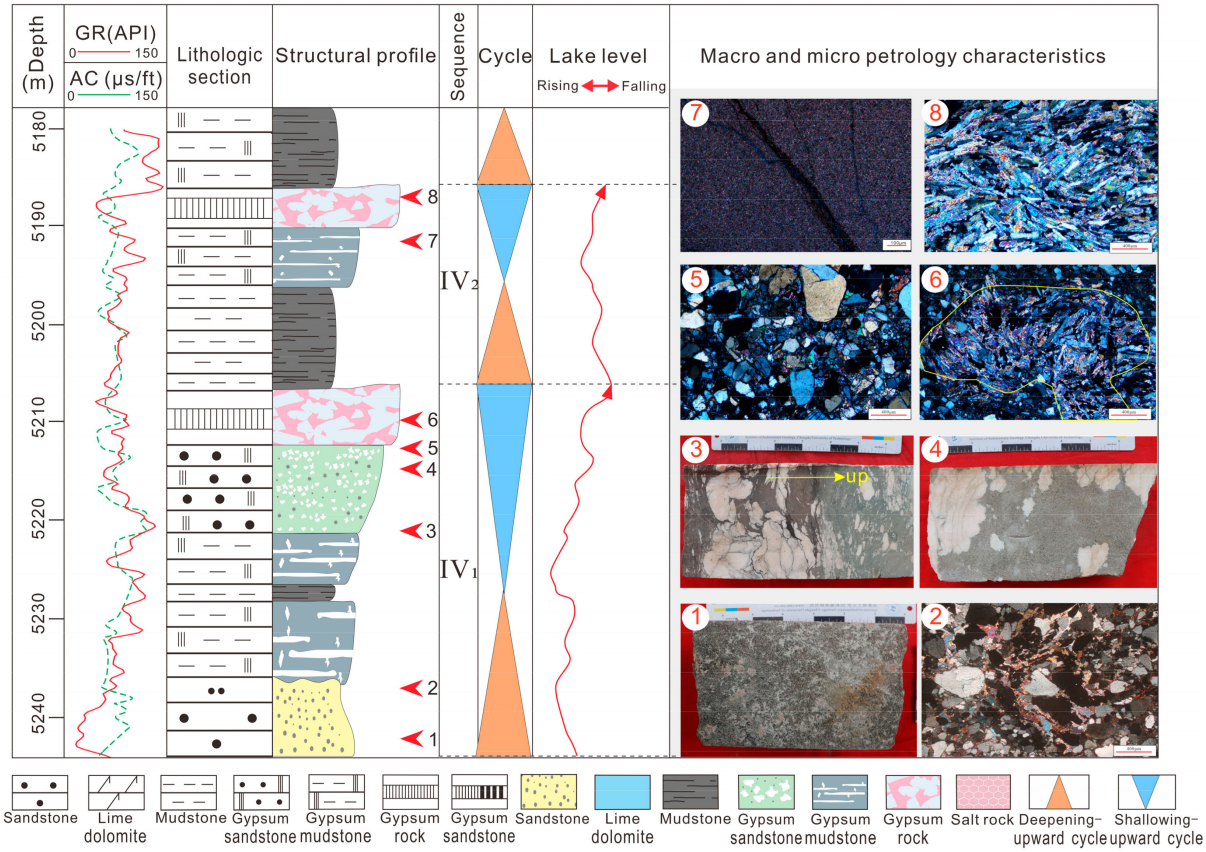

Figure 8. Typical assemblies in the vertical cycle sequence IV of the Kumugeliemu Group (XH3 Well, 5178.5–5243.6 m) in the Xinhe area.

4.4. High-Frequency Cycle Inter-Well Comparison

Multiple types of single cycles are frequently superimposed in the vertical direction, with some differences. By building five wells from west to east in the study area of the Kumugeliemu Group with a cycle structure profile (Figure 9), an evolution model of the study area was established by analysis of the cycle stratigraphic characteristics in terms of stratigraphic thickness, cycle combination differences, and vertical evolution.

The Kumugeliemu Group can be divided into two third-order sequence cycles, and each complete third-order cycle represents a rapid rise–slow decrease process of the lake surface (Figure 3). The study area is influenced by the low bulge of the perimeter of the Yingmaili Uplift and the Wensu Bulge, forming lateral shading, and the subsidence center tends to move westward. The top flattening treatment of the study area (YT10 well–XH3 well–XH5 well–XH1 well–XH101 well) showed that the variation of the thickness difference between the wells could better reflect the evolution of the paleogeomorphology features in the study area by comparing the longitudinal and lateral high-frequency cycles.

After the recognition of the above-mentioned cycle interface and four typical single-cycle features, the high-frequency cycles of each well were constructed from the complete or incomplete single cycles; an average of 22 high-frequency cycles were identified. The bottoms were all marked by carbonate rock development, and most of the cycle tops showed a gypsum sediment. A more uniform thickness of the gypsum salt in the middle was observed, with the thickest sediment in the XH3 well. The average thickness of the study area from west to east gradually decreases, and the number of cycles increases, exhibiting a paleogeomorphology pattern of "west-low–east-high" of the lake basin during the sedimentary period. The thickness of the cycle in the center of the lake basin was greater than that at the edge of the lake basin, indicating that the study area underwent a compensatory–over compensatory deposition process locally in the Tabei Uplift. There

was also a rapid rise in the lake level and an increase in the extension of the lake basin during the lake transgression semi-cycle: when the lake regression semi-cycle occurred, the lake level slowly decreased, and the lake basin area gradually shrank, reflecting the rapid expansion of the overall lake basin subjected to a rapid formation of deposit, followed by gradual evaporation and shrinkage as well as filling and replenishment (Figure 9).

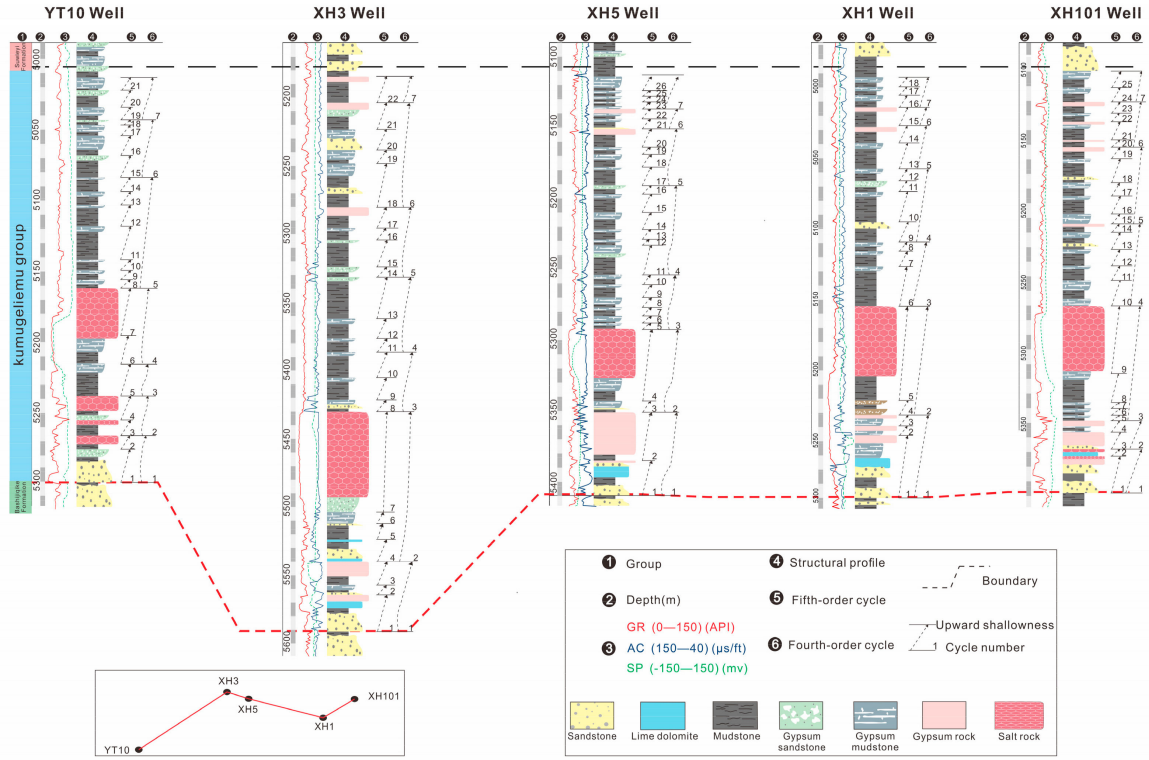

Figure 9. Profile of the framework well cycle structure of the Paleogene Kumugeliemu Group in the Xinhe area.

5. Discussion

5.1. Bottom Structure of the Lake Basin and Supply Direction of Terrestrial Clastic Materials

From the third-order and fourth-order sequence stratigraphic frameworks, the morphology of the lake basin bottom was determined by comparing high-frequency cycles between vertical and horizontal wells and using the differences in cycle thickness among each well in the study area. The so-called bottom morphology of a lake basin refers to the geomorphological characteristics of the bottom of the lake basin during its evolution [4,37]. From the results of high-frequency cycle structure and spatial comparison analysis (Figure 7), the study area showed a sedimentary pattern of "low in the west and high in the east", opposite to the regional background of "high in the west and low in the east", as shown in Figure 9. The lake basin appeared characterized by a low undulating terrain with alternating uplifts and depressions, which is consistent with the 3D seismic facies plane of the study area (Figure 10). Vertically, the thickness of the cycles and the sedimentary differences between each well area gradually decreased, reflecting the evolution of the lake basin during the sedimentary period of the Kumugeliemu Group, which continuously acquired deposited material, gradually salinized, and shrank. This is consistent with previous studies on the Kuqa Depression, indicating certain common features in the region [12,38].

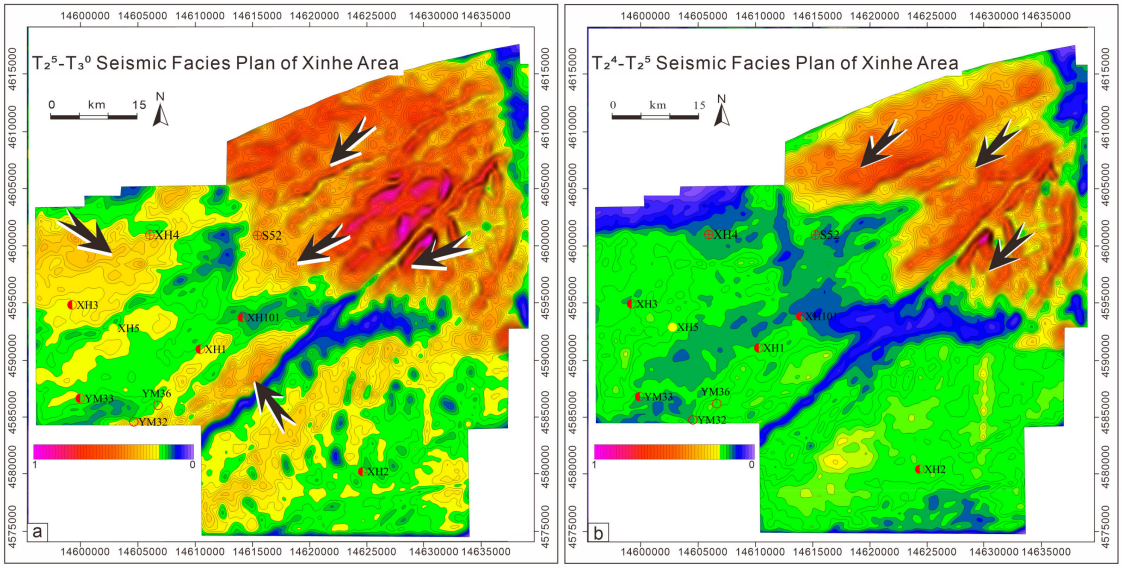

Figure 10. 3D seismic facies plan of the Paleogene Kumugeliemu Group in the study area (the arrows indicate the material source direction). (**a**) T25-T30 Seismic Facies Plan of Xinhe Area; (**b**) T24-T25 Seismic Facies Plan of Xinhe Area.

Based on a previous study, the main sources of sulfate minerals, which are among the main elements forming gypsum salt layers, are both terrestrial sources and water bodies in lake basins [39]. Thus, determining the direction of sources allows also determining the sources of brine ions in the gypsum salt layers in the lake basin [40,41]. From the 3D seismic facies of the study area, it was found that during the T_2^5–T_3^0 period (Figure 10a), very thick strata appeared in the NE direction, and a significant thickening of the strata in the NW and SE directions in the lake basin occurred. The main sedimentary unloading center of the lake was the lake basin slope break zone [42,43], and terrigenous debris provided sedimentation, with a fast sedimentation rate. The interior of the lake basin mainly comprised fine-grained sediments, and the thickness of the rock layers was relatively low; it is believed that the source direction was from the thick layers to the thin layers [44]. Thus, the sedimentation of the lake basin during this period was influenced by multi-directional sources, mainly in the NE direction, and there were also inputs from the NW and SE directions. During the T_2^4–T_2^5 period, the undulation of the lake basin bottom decreased, and the interior became flatter. The total number of sources in the NW and SE directions decreased, with the main source direction still being the NE direction (Figure 10b). Based on the bottom shape of the lake basin and the direction of the source, it is believed that the Kumugeliemu Group in the study area was influenced by the Tianshan orogenic belt during the period, and the origin was mainly in the NE direction.

5.2. Analysis of the Causes of the High-Frequency Lake Level Fluctuations

Lakes have a much smaller water body area than the ocean; hence, they are more sensitive to the climate than the ocean. Thus, the lake level changes at a higher frequency than the sea level. Lake water supply and evaporation are jointly affected by the ancient climate, thereby controlling the high-frequency changes in a lake level [45]. The changes in a lake level are also the most intuitive manifestation of climate change.

In the early Paleogene, the Tarim Basin, due to the remote effect of the Indo–European plate collision and early Himalayan tectonic movement, pushed the Kunlun, Altun, and Tianshan orogenic belts around the basin, compressing and activating them, and then uplifted them again (Figure 1a) [46–52], forming a natural "barrier" which hindered the warm and humid Indian Ocean monsoon from the southwest of the basin [53]. The impact of this airflow on the interior of the basin gradually decreased, causing the climate

in the region to slowly transform into a dry and evaporative paleoclimate during the Paleogene period.

Research on the Himalayas' elevation showed that the sea level was about 1000 m before 55–50 Ma, and then slowly increased to 2300 m before 21–19 Ma, reaching its current height only 5–7 Ma ago [54]. The Kumgeliemu sedimentation (33.9–66 Ma) period [34,55,56] occurred in the low-altitude period of the Himalayas. The Tarim Basin is not a completely closed basin, and the surrounding mountains do not completely protect it from the climate variations between the inside and the outside of the basin. Simultaneously, influenced by the continuous water supply from the surrounding mountain and fresh water supply, it is more characterized by a semi-closed–semi-open pattern. Therefore, the frequent fluctuations of the lake level may be influenced by the alternating warm climate in the southwest and dry and cold climate in the north. At the same time, during the sedimentation of the early Paleogene Kumugeliemu Group in the Xishan Mountains, normal faults continued to develop, generally along the position of reverse faults, which is a typical negative inversion feature [57]. During the Paleogene (Paleocene–Early Eocene), the world was in the Paleocene–Eocene thermal maximum (PETM) extreme hot period, which was one of the most important global extreme drought climate events in the Cenozoic era [58–60]. The salt structural cover of the Kumegeliemu Group in the study area was widely developed and affected by this event.

The study area showed a typical sedimentary process of rapid lake invasion and slow lake retreat, with a single-cycle thickness typically ranging from a few meters to several tens of meters. Ignoring the short-term structural influence, the sedimentary thickness of a cycle can be used to approximate the sedimentary depth of the cycle. The average thickness difference of each well area in the study area was also small, not exceeding 8 m (Figure 9), which also reflects the small terrain differences within the lake basin during this sedimentary period. The above characteristics showed that evaporite was widely developed in the study area, mainly developing a coastal shallow-lake evaporation tidal flat shallow-water sedimentary system, and the depth of the sedimentary water was not different; it showed similar characteristics to those of modern evaporite deposition and most salt minerals in geological history [61,62]. The main study area showed a lithology of clastic rock–carbonate–sulfate rock–salt rock, and the complete sedimentary stage can be roughly divided into the following (Figure 11):

1. Freshwater sedimentation stage (Figure 11a): during the rapid lake invasion period, the lake basin expanded, the climate was relatively humid, and fresh water and seasonal river water flew into the lake. At this moment, there was relatively low salinity, with the continuous input of terrigenous detrital materials and relatively fewer chemical sediments. The settlement center in the study area mainly comprised fine sediments (siltstone and mudstone), with developed shoal bars. The positive-grain sequence structure was seen in siltstone, the laminar structure was seen in mudstone, and horizontal bedding was also observed. The overall grain size became fine from bottom to top, showing a positive rhythm, which is the main feature of the coastal shallow lake sedimentary system. The sediment thickness gradually became thinner from the center of the lake basin to the edge of the lake basin, reflecting the characteristic of the supply of terrigenous clastic materials gradually decreasing with the increasing of the hydrodynamic force.
2. Brackish water depositional stage (Figure 11b): as the climate gradually became dry and hot, the relative lake level began to decline, the fresh water supply started to decrease, the evaporation gradually increased, the salinity gradually increased, the lake water gradually became salty, and the content of Ca^{2+} and Mg^{2+} gradually increased, forming carbonate deposits (limestone, micrite limestone); a thin layer of argillaceous terrigenous clastic materials was seen locally, and a small amount of evaporated minerals were separated locally. As a paste patch, the water environment gradually transitioned from a reducing environment to an oxidizing environment.

3. Saltwater depositional stage (Figure 11c): the climate continued to be dry and hot, the evaporation was greater than the fresh water supply, the lake basin scope gradually shrank, the degree of salinization of the lake water continued to increase, sulfate rock began to precipitate, and heavy brine gradually formed. Several gypsum blocks developed in clastic rock, and the particle size of the blocks gradually increased. Gypsum siltstone and gypsum mudstone were the main lithology. A large gypsum layer developed at the top of this sedimentary stage, while gypsum flats and salt flats locally developed in the lake basin.
4. Salt lake depositional stage (Figure 11d): at this time, the evaporation was far greater than the fresh water supply, and the lake basin continued to shrink with the enhancement of evaporation, showing the characteristics of a "teardrop" salt lake. The lake level continued to decline, and the heavy brine continued to infiltrate due to gravity. The salinity of the lake water deepened and increased, and rock salt crystals continued to precipitate. A large salt layer developed, with a thickness of several tens of meters. Local gypsum flats and salt flats gradually formed a wide and gentle lagoon.
5. Semi-saltwater depositional stage (Figure 11e): affected by the Himalayan movement, the Kuqa Depression activity began to activate, and the uplift of the Tianshan orogenic belt brought back terrigenous debris. Surface runoff began to be transported again and merge into the lake basin. Affected by the lake intrusion and retreat events, a set of sandstone and mudstone interbedded sediments were deposited in the study area. Affected by the seasonal monsoon climate, the surface runoff decreased during the drought stage, the transportation capacity deteriorated, the lake basins shrank, brackish water deposition was experienced, and gypsum–mudstone layers developed. During the humid stage, the surface runoff increased, the transportation capacity augmented, and the lake basin expanded again, forming freshwater lake basin sedimentation and developing sandstone layers.

In summary, the structure and paleoclimate mainly affected the evolution of the lake basin in the Kumugeliemu Group in the study area. The salt lake experienced the evolution sequence of clastic rock sedimentation, carbonate sedimentation, sulfate sedimentation, and halite crystal precipitation. The sedimentation period experienced was characterized by rapid lake invasions, an expanded lake basin, and an increased accommodating space. The freshwater supply carried a large amount of terrigenous clastic material, while providing the salt minerals required for the formation of gypsum salt rocks. The lake retreated slowly, the lake basin shrank, and the accommodation space decreased. Lake water evaporation was greater than water recharging. The lake water evaporated and concentrated, and the salt minerals were separated based on their solubility. The development of thick salt rocks in the Xinhe area was due to the frequent and continuous "evaporation and concentration" of the lake water, and the continuous infiltration of heavy brine, leading to an increase in salinity. The evolution and development of salt lakes underwent multiple cyclic sequences, and the complete sedimentary sequence determined the evolution from coastal shallow lake formation, to early salt lake development, to wide and gentle lagoon formation, to late salt lake development, and finally to salt lake extinction. During this period, the unique sedimentary model led to a good reservoir cap combination of the sedimentary gypsum salt layer and the underlying sandstone.

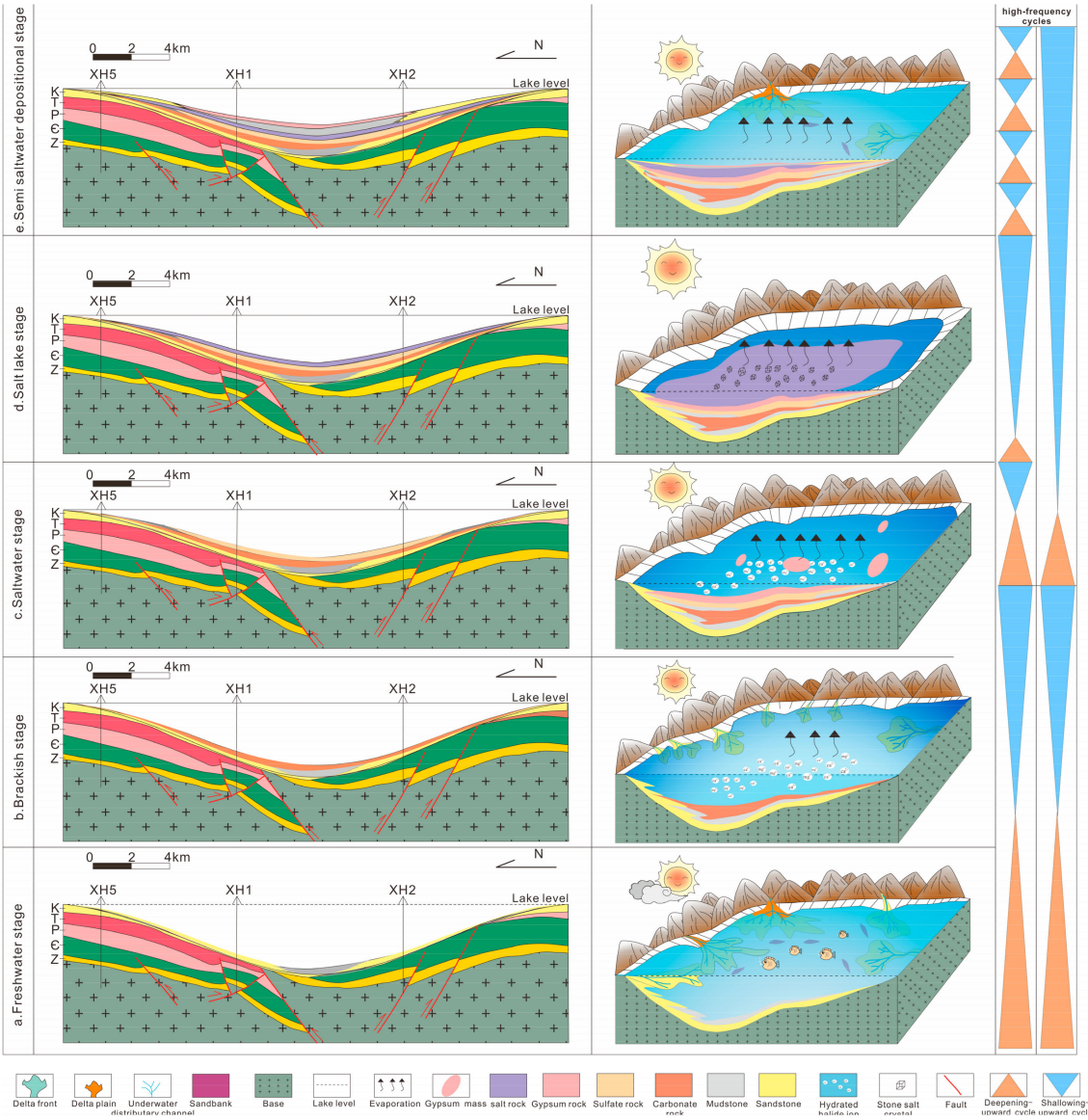

Figure 11. Tectonic evolution and sedimentary model map of the Paleogene Kumugeliemu Group Lake Basin in the Xinhe area.

6. Conclusions

(1) From the drilling cores, logging curves, and 2D seismic log data, three sets of marker layers were found as isochronous comparison layers, namely, a paste mudstone component, a gypsum salt component, and a carbonate component, which showed continuity with the surrounding edge of the Wensu Bulge. They were further divided into four components: a bottom sandstone component ($E_{1\text{-}2}$ km^1), a lower paste mudstone component ($E_{1\text{-}2}$ km^2), a gypsum salt component ($E_{1\text{-}2}$ km^3), and an upper paste mudstone component ($E_{1\text{-}2}$ km^4): they formed two third-level orders (ESQ_1, ESQ_2), which were further divided into seven fourth-level orders (Esq1–Esq7).

(2) The Kumugeliemu Group as a whole is an arid and saline lacustrine sedimentary system. The internal rock formation frequently changes with periodic vertical superposition, with laminated gypsum salt, gypsum mudstone, and gypsum rock as the cycle boundaries. Each single cycle mainly showed an upward-shallowing sedimentary sequence of rapid lake transgression–slow lake regression, constituting a typical cycle structure of massive sandstone–laminated mudstone–lime dolomite–gypsum rock, mas-

sive sandstone–laminated mudstone–gypsum sand (mud) rock (salt rock), and massive sandstone–massive paste mud (sand) rock–gypsum rock.

(3) Each single cycle was superimposed into different complete or incomplete sedimentary cycles, and the cycle structure profile of five wells was built laterally from west to east in the Kumugeliemu Group of the study area. Using the inter-well spinning thickness difference, it was found that the spinning thickness difference gradually decreased vertically, and the number of cycles increased from west to east. This indicated that the study area has a paleogeomorphology pattern of "west low and east high", and small geomorphological differences.

(4) The main controlling factor of the high-frequency cycles in the lake basin of the study area appeared to be the climate, with relatively static structures. However, due to the influence of the Himalayan movement, it brought from the NE direction terrigenous debris material, which was the main source of sandstone sedimentation. The lake basin underwent a typical sedimentary process of rapid lake invasion and slow lake retreat and experienced five sedimentary stages: fresh water, brackish water, salt water, saline lake, and semi-saline water, reflecting the evolutionary process of increasing salinity, continuous filling of the lake basin, and gradual salinization and shrinkage.

Author Contributions: Conceptualization, J.T. and Y.Y.; methodology, X.Z.; software, Y.L.; validation, Y.Z. and Q.X.; writing—original draft preparation, Y.Y.; writing—review and editing, J.T. and X.Z. All authors have read and agreed to the published version of the manuscript.

Funding: This research received no external funding.

Data Availability Statement: Data will be made available on request.

Acknowledgments: The careful reviews and constructive suggestions of the manuscript by anonymous reviewers are greatly appreciated.

Conflicts of Interest: The authors declare no conflict of interest.

References

1. Lin, X.X.; Hou, Z.J. A quantitative analysis research on relative lacustrine level changes in the Lower Cretaceous Fuyu reservoir in the Songliao Basin. *J. Stratigr.* **2014**, *38*, 170–180.
2. Tapponnier, P.; Xu, Z.; Roger, F. Oblique Stepwise Rise and Growth of the Tibet Plateau. *Science* **2001**, *294*, 1671–1678. [CrossRef] [PubMed]
3. Zhang, Y.S.; Wu, K.Y.; Jiang, Y.H.; Wang, P.; Cai, Z.H.; Gao, F.R.; Tan, W.; Gao, S.; Xian, B.Z. Geological characteristics of deep carbonate hydrocarbon-bearing pool in the western Yingxiongling area in Qaidam Basi. *Nat. Gas Geosci.* **2018**, *29*, 358–369.
4. Qiao, Y.P.; Tan, X.C.; Liu, Y.; Xiong, Y.; Wu, K.Y.; Zhang, Y.S.; Yang, B.; Ren, L. Characteristics of High—frequency Lake—level Fluctuations in the Saline Lacustrine Basin and Its Geological Significance: A case study from the upper member of the Paleogene Lower Ganchaigou Formation in the Yingxi area, Qaidam Basin. *Acta Sedimentol. Sin.* **2020**, *38*, 1152–1165.
5. Guo, R.T.; Zhang, Y.S.; Chen, X.D.; Zhang, Q.H.; Wang, P.; Cui, J.; Jiang, Y.H.; Li, Y.F.; Jiang, Q.C.; Liu, B. High frequency cycles and paleogeomorphic characteristics of upper member of Lower Ganchaigou Formation in Yingxi area, Qaidam Basin. *Acta Sedimentol. Sin.* **2019**, *37*, 812–824.
6. Xiong, Y.; Wu, K.Y.; Tan, X.C.; Zhang, Y.S.; Yang, B.; Ren, L.; Liu, L.; Liu, Y.; Qiao, Y.P.; Wang, X.F. Influence of lake-level fluctuation on the mixed saline lacustrine carbonate reservoir: A case study from the Upper Member of Paleogene Lower Ganchaigou Formation in the Yingxi area of Qaidam Basin. *J. Palaeogeogr.* **2018**, *20*, 855–868.
7. Zhu, D.Y.; Wang, Y.; Yin, Y.; Yang, W.Q.; Zhu, D.S.; Ning, F.X. Study on the relationship between saline environmental deposition and shale oil-gas in faulted basin: A case study of areas of Dongying sag and Bonan subsag. *Pet. Geol. Recovery Effic.* **2015**, *22*, 7–13.
8. Zhou, J.H.; Xian, B.Z.; Zhang, J.G.; Zhong, Q.; Chen, P. Organic matter enrichment law of lacustrine shale constrained by high resolution cyclostratigraphy: A case study from the lower sub-member of Member 3 of Paleogene Shahejie Formation, Dongying sag. *J. Palaeogeogr.* **2022**, *24*, 759–770.
9. Wu, J.; Zhu, C.; Yang, G.; Zhao, J.L.; Gong, Q.S.; Song, G.Y. High-resolution sequence stratigraphy characteristics and sedimentary facies evolution of thin sands under high frequency lake level change: A case study of lower sand member of Paleogene Kumugeliemu Group in margin of Wensu Uplift-Yingmaili Uplift area. *Pet. Geol. Recovery Effic.* **2020**, *27*, 38–46.
10. Wang, B.; Lei, G.L.; Wu, C.; Mo, T.; Zhou, P.; Shang, J.W.; Xie, Y.; Li, M.Y. Division and sedimentary models for the Palaeogene gypsum mudstones in the Kuqa depression, Xinjiang. *Sediment. Geol. Tethyan Geol.* **2016**, *36*, 60–65.
11. Cao, Y.T.; Liu, C.L.; Yang, H.J.; Gu, Q.Y.; Jiao, P.C.; Lu, Y.H. Identification and correlation of Paleogene and Neogene evaporite sedimentary cycles of in Kuqa Basin, Xinjian. *J. Palaeogeogr.* **2010**, *12*, 31–41.

12. Cao, Y.C.; Jiang, Z.X.; Xia, B.; Yang, W.L. Characteristics and controlling factors of T-R sequence in continental deposits of rift basin: An example from the Dong Ying depression, Eastern China. *Chin. J. Geol.* **2004**, *1*, 111–122.
13. Zhang, D.Z.; Ji, Y.L.; Zhang, R.F.; Chu, L.L.; Ni, C.; Wang, L. Research on the Sequence Stratigraphy of Eogene in Raoyang Depression. *Geol. Surv. Res.* **2008**, *31*, 33–42.
14. Zhang, T.; Zhang, C.M.; Qu, J.H.; Zhu, R.; Yuan, R. Identification and comparison of high-frequency sedimentary cycles based on Milankovitch theory: A case study of Baikouquan Formation in Mahu Sag, Junggar Basin. *J. Northeast Pet. Univ.* **2017**, *41*, 54–61.
15. Liu, C.S.; Guo, J.H.; Guo, S.Z. sequence stratigraphy study of Paleogene in Tarim Basin. *J. Northwest Univ.* **2012**, *42*, 813–818.
16. Shao, L.Y.; He, Z.Z.; Gu, J.Y.; Luo, W.L.; Jia, J.H.; Liu, Y.F.; Zhang, L.J.; Zhang, P.F. Lithofacies Paleogeography of the Paleogene in Tarim Basin. *J. Palaeogeogr.* **2006**, *8*, 353–364.
17. Lv, X.X.; Jin, Z.J.; Zhou, X.Y.; Yang, M.H.; Ma, Y.J.; Zhang, C. Oil and gas exploration prospect in wushi sag and wensu uplift of Tarim Basin. *J. China Univ. Pet.* **2006**, *30*, 17–21+25.
18. Jiao, Z.F.; Gao, Z.Q. Formation, evolution and Hydrocarbom-Controlling geological conditions of Major Paleohighs, Tarim Basin. *Nat. Gas Geosci.* **2008**, *19*, 639–646.
19. Wang, J.P.; Zhang, H.L.; Zhang, R.H.; Yang, X.J.; Zeng, Q.L.; Chen, X.G.; Zhao, J.Q. Enhancement of ultra-deep tight sandstone reservoirs by fracture A case study of Keshen Gas Field in Kuqa Depression, Tarim Basin. *Oil Gas Geol.* **2018**, *39*, 77–88.
20. Zhang, G.Y.; Xue, L.Q. Petroleum distribution and exploration direction in foreland basins in central and western China. *Pet. Explor. Dev.* **2002**, *29*, 1–5+9.
21. Liu, J.Y.; Wang, Q.H.; Lin, C.S.; Zhang, L.J.; Lei, Y.P.; Hu, G.C.; Hu, B. Sequence, and system tract of Paleogene Kumugeliemu Group in western Kuqa Depression. *Pet. Explor. Dev.* **2008**, *35*, 651–656. [CrossRef]
22. Wang, Z.Q.; Liu, B.; Hu, Z.Y.; Wang, X. High-resolution sequence stratigraphic framework and sedimentary characteristics of Nantun Formation in Sudeerte area of Hailar Basin. *Pet. Geol. Oilfield Dev. Daqing* **2019**, *38*, 7–14.
23. Chen, Y.Q.; Wang, X.X.; He, H.; Yi, Y. Evolution of uplift and depression framework of Tarim Craton in Nanhua-Cambrian. *China Pet. Explor.* **2022**, *27*, 30–46.
24. Zhai, M.G. The main old lands in China and assembly of Chinese unified continent. *Sci. China Ser. D Earth Sci.* **2013**, *56*, 1829–1852. [CrossRef]
25. Jia, C.Z. Structural Characteristics and Oil/Gas Accumulation Rules of the Tarim Basin. *Xinjiang Pet. Geol.* **1999**, *20*, 3–9+94.
26. Tang, L.J.; Jin, Z.J. Negative inversion process and hydrocarbon accumulation of Yaha fault zone in northern uplift, Tarim Basin. *J. Sedimentol.* **2000**, *18*, 302–309.
27. Jin, Z.J.; Zhang, Y.W.; Chen, S.P. Tectonic sedimentary wave process in the Tarim Basin. *Chin. Sci. Part D Earth Sci.* **2005**, *35*, 530–539.
28. Zheng, J.F.; Shen, A.J.; Qiao, Z.F.; Wu, X.N.; Zhang, T.F. Characteristics, and pore genesis of dolomite in the Penglaiba Formation in Keping Bachu outcrop area. *J. Pet.* **2014**, *35*, 664–672.
29. Liu, Y.F.; Xia, H.; Sun, Q.; Lin, C.S.; Zhao, H.T.; Li, H.; Huang, L.M.; Zhang, Z.Y. Sequence stratigraphy and Sedimentary evolution of Bashijiqike Formation in the west of Tabei Uplift, Tarim Basin. *Nat. Gas Geosci.* **2019**, *30*, 62–73.
30. Wang, T.; Wu, M.M.; Cheng, R.H.; Wang, B.; Xu, Z.Z.; Yao, K.; Wang, X.Y. Cyclic gas injection development of condensate gas reservoir with destiny and meaning—Strata movement in YaHa condensate field, for example. In Proceedings of the International Conference on Oil and Gas Field Exploration and Development, Chengdu, China, 16–18 October 2019; pp. 1458–1467.
31. Guo, L.Z.; Shi, Y.S.; Lu, H.F. Two long-range effects of Indo Tibetan collisions. In *Collected Works on Modern Geology*; Nanjing University: Nanjing, China, 1992; pp. 1–7.
32. Hong, C.J.; Kang, R.D.; Zhou, F.F.; Fei, J.W.; Fang, X.H. Sedimentary characteristics of Cretaceous Bashigei Formation in Xinhe-Sandaoqiao area. *Xinjiang Geol.* **2016**, *34*, 230–234.
33. He, C.F.; Zhang, X.; Tian, J.C.; Xia, Y.T.; Yang, Y.R.; Chen, J.; Wang, X.Y. Sedimentary facies and sedimentary model of thin sand bodies of Lower Cretaceous Shushanhe Formation in Xinhe Area, Northern Tarim Basin. *Lithol. Reserv.* **2023**, *35*, 120–131.
34. Xi, D.P.; Tang, Z.H.; Wang, X.J.; Qin, Z.H.; Cao, W.X.; Jiang, T.; Wu, B.X.; Li, Y.H.; Zhang, Y.Y.; Jiang, W.B.; et al. Cretaceous Paleogene marine stratigraphic framework and records of major geological events in the western Tarim Basin. *Geosci. Front.* **2020**, *27*, 165–198.62.
35. Zhang, L.J.; Wang, Y.H.; Gu, Q.Y. Sedimentary reservoir characteristics of Carboniferous I oil formation in Lunnan area, Tarim Basin. *Xinjiang Geol.* **2002**, *20*, 276–277.
36. Deng, H.W. Application of high-resolution sequence stratigraphy. *J. Palaeogeogr.* **2009**, *11*, 471–480.
37. Wei, K.S.; Xu, H.D.; Ye, S.F.; Guo, Z.; Xu, H.; Ren, Y.; Wang, Y. High-resolution sequence stritigraphic framework in Cretaceous, Songliao Basin. *Oil Gas Geol.* **1997**, *18*, 9–16.
38. Ma, T.; Ma, Q.; Wang, Z.Y.; Yuan, C.; Hu, J.F.; Wang, H. Sequence stratigraphic framework and sedimentary evolution of Paleogene prototype Sedimentary basin in Kuqa Depression. *Geol. Sci.* **2020**, *55*, 369–381.
39. Raab, M.; Spiro, B. Sulfur isotopic variations during seawater evaporation with fractional crystallization. *Chem. Geol. Isot. Geosci. Sect.* **1991**, *86*, 323–333. [CrossRef]
40. Han, N.N. *Evaporitic Rock's Characteristics of Paleogene-Neogene in Kuqa Basin and Its Relations with Paleo-Environment*; China University of Geosciences: Beijing, China, 2007.
41. Zhang, H.; Song, C.Z. Geochemical Characteristics of Loess-Palaeosols from the Northern Slope of Dabie Mountain and Research of Its Provenance in the Enrichment Factor Way. *Geol. Sci. Technol. Inf.* **2013**, *32*, 87–93.

42. Lin, C.S.; Pan, Y.L.; Xiao, J.X.; Kong, F.X.; Liu, J.Y.; Zheng, H.R. Structural slope break zone—An important concept for sequence analysis and oil and gas prediction in fault basins. *Earth Sci.* **2000**, *25*, 260–266.
43. Liu, H.; Tian, L.X.; Zhou, X.H.; Zhu, C.M. Slope break systems of rift lacustrine basin and erosion-depositional response: A case study of the Paleogene in Huanghekou sag, Bohai sea. *China Offshore Oil Gas* **2017**, *29*, 28–38.
44. Xu, C.G.; Lai, W.C.; Xue, Y.A.; Yu, S.; Cheng, J.C. Application of paleogeomorphological analysis in predicting Paleogene reservoirs in the Bohai Sea. *Pet. Explor. Dev.* **2004**, *31*, 53–56.
45. Wu, W.; Lin, C.S.; Zhou, X.H.; Li, Q.; Xing, Z.C.; Yan, Y. Paleoclimate evolution and its influence on lake level changes of Paleogene Dongying Ep-och in Liaodong Bay, East China. *J. China Univ. Pet.* **2012**, *36*, 33–39.
46. Molnar, P.; Tapponnier, P. Cenozoic tectonics of Asia: Effects of a continental collision. *Science* **1975**, *189*, 419–426. [CrossRef] [PubMed]
47. Tapponnier, P.; Molnar, P. Active faulting and tectonics in China. *J. Geophys. Res.* **1977**, *82*, 2905–2930. [CrossRef]
48. Hendrix, M.S.; Dumitru, T.A.; Graham, S.A. Late Oligocene-early Miocene unroofing in the Chinese Tian Shan: An early effect of the India-Asia collision. *Geology* **1994**, *22*, 487–490. [CrossRef]
49. Yin, A.; Nie, S.; Craig, P.; Harrison, T.M.; Ryerson, F.; Yang, G. Late Cenozoic tectonic evolution of the southern Chinese Tian Sha. *Tectonics* **1998**, *17*, 1–27. [CrossRef]
50. Charreau, J.; Chen, Y.; Gilder, S.; Barrier, L.; Dominguez, S.; Augier, R.; Sen, S.; Avouac, J.-P.; Gallaud, A.; Graveleau, F.; et al. Neogene uplift of the Tian Shan Mountains observed in the magnetic record of the Jingou River section (northwest China). *Tectonics* **2009**, *28*, 224–243. [CrossRef]
51. Tang, X.; Yang, S.; Hu, S. Thermal and maturation history of Jurassic source rocks in the Kuqa foreland depression of Tarim Basin, NW China. *J. Asian Earth Sci.* **2014**, *89*, 1–9. [CrossRef]
52. Laborde, A.; Barrier, L.; Simoes, M.; Li, H.; Coudroy, T.; Van der Woerd, J.; Tapponnier, P. Cenozoic deformation of the Tarim Basin and surrounding ranges (Xinjiang, China): A regional overview. *Earth-Sci. Rev.* **2019**, *197*, 102–891. [CrossRef]
53. Kent-Corson, M.; Ritts, B.; Zhuang, G.; Bovet, P.M.; Graham, S.A.; Chamberlain, C.P. Stable isotopic constraints on the tectonic, topographic, and climatic evolution of the northern margin of the Tibetan Platea. *Earth Planet. Sci. Lett.* **2009**, *282*, 158–166. [CrossRef]
54. Ding, L.; Spicer, R.A.; Yang, J.; Xu, Q.; Cai, F.; Li, S.; Lai, Q.; Wang, H.; Spicer, T.E.V.; Yue, Y.; et al. Quantifying the rise of the Himalaya orogen and implications for the South Asian monsoon. *Geology* **2017**, *45*, 215–218. [CrossRef]
55. Zeng, L.; Wang, H.; Gong, L.; Liu, B. Impacts of the tectonic stress field on natural gas migration and accumulation: A case study of the Kuqa Depression in the Tarim Basin, China. *Mar. Pet. Geol.* **2010**, *27*, 1616–1627. [CrossRef]
56. Zhang, J.Y. *Paleogene Paleogeographic Reconstruction of the Paleogene Tarim Basin (NW China) and Sedimentary Response*; China University of Geosciences: Wuhan, China, 2022.
57. Li, T.; Tong, W.J.; Hu, Z.G.; Ding, H.; Liang, L.X. Paleogene Cretaceous hydrocarbon accumulation model in the northern Sandaoqiao area of the Tarim Basin. *J. Yangtze Univ.* **2023**, *2*, 1–12.
58. Zachos, J. Trends, Rhythms, and Aberrations in Global Climate 65 Ma to Present. *Science* **2001**, *292*, 686–693. [CrossRef]
59. Cramer, B.S.; Toggweiler, J.R.; Wright, J.D.; Katz, M.E.; Miller, K.G. Ocean overturning since the Late Cretaceous: Inferences from a new benthic foraminiferal isotope compilation. *Paleoceanography* **2009**, *24*, 4216–4230. [CrossRef]
60. Morón, S.; Fox, D.L.; Feinberg, J.M.; Jaramillo, C.; Bayona, G.; Montes, C.; Bloch, J.I. Climate change during the Early Paleogene in the Bogotá Basin (Colombia) inferred from paleosol carbon isotope stratigraphy, major oxides, and environmental magnetism. *Palaeogeogr. Palaeoclimatol. Palaeoecol.* **2013**, *388*, 115–127. [CrossRef]
61. Gao, H.C.; Chen, F.L.; Liu, G.R.; Liu, Z.F. Advances, problems and prospect in studies of origin of salt rocks of the Paleogene Shahejie Formation in Dongpu Sag. *J. Palaeogeogr.* **2009**, *11*, 251–264.
62. Yuan, J.Q.; Xi, J.K. Problems of palaeogeography and lithofacies of evaporites. *Geol. Shanxi* **1985**, *3*, 1–13.